

Photochemical Oxidation of Polyethylene Glycol in Aqueous Solution by UV/H₂O₂ with Steel Waste

Chyow-San Chiou^[1]

Department of Environmental Engineering, National I-Lan University
I-Lan 260, Taiwan

Yi-Hung Chen^[2]

Department of Chemical and Material Engineering, National Kaohsiung University of Applied Sciences
Kaohsiung 807, Taiwan

Ching-Yuan Chang^[3]

Graduate Institute of Environmental Engineering, National Taiwan University
Taipei 106, Taiwan

Je-Lueng Shie^[4], Cheng-Chung Liu^[5], and Chang-Tang Chang^[6]

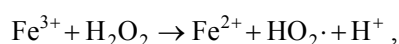
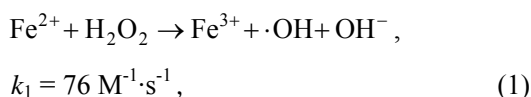
Department of Environmental Engineering, National I-Lan University
I-Lan 260, Taiwan

Abstract—This study evaluated the performance of the photo-Fenton reaction when it was initiated using UV/H₂O₂ with steel waste and basic oxygen furnace slag (BOF slag), here called the UV/H₂O₂/BOF slag process, in order to decompose polyethylene glycol (PEG) in aqueous solution. The concentration of total organic carbon (TOC) was chosen as a mineralization index of the decomposition of PEG in the UV/H₂O₂/BOF slag process. A first-order kinetic model with respect to TOC was appropriately adopted to represent the mineralization of PEG in the UV/H₂O₂/BOF slag process. The experimental results obtained in this study suggest that dosages with 2.49×10^{-4} mol/min-L H₂O₂ and 25 g/L BOF slag loading in a solution at pH = 2.5 with 120 μ W/cm² UV provided the optimal operation conditions for the mineralization of PEG, yielding 79.5% mineralization efficiency after 90 min of reaction time.

Key Words : Photo-Fenton, Mineralization, Basic oxygen furnace slag, UV/H₂O₂, Polyethylene glycol

INTRODUCTION

The application of the Fenton reaction to produce hydroxyl radicals for decomposing organic pollutants has attracted much attention from researchers (Walling, 1975). It has been successfully applied to degrade aromatic compounds (Rivas *et al.*, 2001; Saxe *et al.*, 2000). Through the function of the agent of the Fenton reaction, which is a mixture of H₂O₂ with iron salts, strong oxidative hydroxyl radicals, that is, \cdot OH, can be generated according to the following reactions (Chen and Pignatello, 1997; Tuba and Gurol, 2002) :



$$k_2 = 0.02 \text{ M}^{-1} \cdot \text{s}^{-1} . \quad (2)$$

A Fenton reaction can also be initiated by a heterogeneous catalyst. Iron oxide has recently been employed as a catalyst for oxidizing organic contaminants with hydrogen peroxide (Lin and Gurol, 1998). For example, α -Fe₂O₃ (Watts *et al.*, 1997) and a novel supported γ -FeOOH catalyst (Chou *et al.*, 2001) have been applied, respectively, in the oxidation of chlorobenzenes and benzoic acid with H₂O₂ in aqueous solutions.

In order to enhance the Fenton reaction, a photo-Fenton process (Feng *et al.*, 2003; Liou *et al.*, 2004) was developed by introducing ultraviolet (UV) light into a Fenton process. When UV light is applied,

^[1] 邱求三, To whom all correspondence should be addressed

^[2] 陳奕宏

^[3] 張慶源

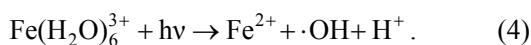
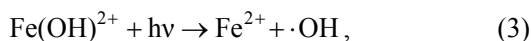
^[4] 謝哲隆

^[5] 劉鎮宗

^[6] 張章堂



Fe^{2+} can be regenerated via the following photo reactions (Wu and Deng, 2000):



The reduction of Fe^{3+} to Fe^{2+} is advantageous for performing a Fenton reaction repeatedly without continuously adding Fe^{2+} . The reaction mechanisms in Eqs. (3) and (4) also regenerate a strong oxidant, $\cdot\text{OH}$. Furthermore, a hydrogen peroxide can produce two hydroxyl radicals initiated by UV light, according to Eq. (5):



Among these routes, Eqs. (3), (4) and (5) facilitate the formation of hydroxyl radicals and increase the decomposition rates of organic compounds. Many previous studies have shown that various refractory organic compounds (Bajt *et al.*, 2001; Kiwi *et al.*, 1994; Lei *et al.*, 1998; Zhao *et al.*, 2004) can be effectively decomposed via the photo-Fenton process.

Basic oxygen furnace slag (BOF slag) is one of the solid wastes that results from the making steel process. The main constituents of BOF slag are CaO , SiO_2 , Fe_2O_3 , FeO , MgO , and MnO . From 5 to 20% FeO and from 1 to 8% Fe_2O_3 are present in BOF slag (Chiou *et al.*, 2004a, 2004b; Li, 1999). Therefore, BOF slag has excellent potential for use in the Fenton and photo-Fenton processes as an iron source due to its abundant iron-containing property. This can facilitate the reuse of waste materials and compliance with environmental regulations.

In the electroplating solutions used by the printed wiring board (PWB) industry, polyethylene glycol (PEG) is used as a sheen and stabilization agent. This study assessed the function of BOF slag in enhancing the UV/ H_2O_2 process, here called the UV/ H_2O_2 /BOF slag process, for mineralizing PEG. The concentration of total organic carbon (TOC) was chosen as a mineralization index of the decomposition of PEG using this UV/ H_2O_2 /BOF slag process. The effects of the pH value, UV intensity, H_2O_2 dosage rate, BOF slag concentration, and reaction temperature on the mineralization of PEG were examined. Related kinetic equations were also developed based on the observed experimental results.

MATERIALS AND METHODS

PEG ($\text{H}(\text{OCH}_2\text{CH}_2)_n\text{OH}$) used in this study was purchased from Merck (Darmstadt, Germany) and was reagent grade with a molecular weight (MW) of 5,000 to 7,000. Hydrogen peroxide (35 wt%) was supplied by the Shimakyu Co. (Japan). BOF slag was

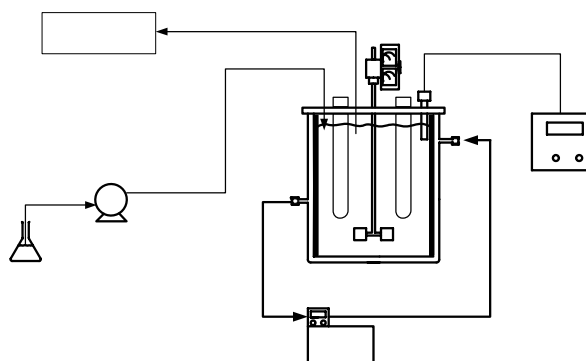


Fig. 1. The experimental apparatus. Components: (1) syringe pump, (2) reaction vessel, (3) UV lamp, (4) stirrer, (5) pH meter, and (6) thermostat.

obtained from the China Steel Corp., Taiwan. The BOF slag was washed with distilled water to remove adhering dust and then dried at 103°C . The heated BOF slag was cooled and sieved with No. 10 (opening 2 mm) and No. 18 (opening 1 mm) mesh sieves to ensure a specific particle size of each sample. The TOC of each sample was analyzed with a TOC analyzer (Tekmar Dohrmann Phoenix 8000).

Oxidation reaction batch experiments were conducted in a 2-L round-bottle glass flask (9 cm diameter and 32 cm height) with a water jacket (see Fig. 1). Mixing was performed by a variable speed motor connected to a stainless steel shaft, and the speed was kept at 400 rpm during the whole reaction time. The UV irradiation sources were two 8 W lamps encased in a quartz tube with wavelengths of 312 nm. The UV intensity of one 8 W UV lamp was $60 \mu\text{W}/\text{cm}^2$, and which was detected by a UVX Radiometer (UVP Inc., U.S.A.) attached on the outside surface of the encased quartz tube. A variable speed motor connected to a stainless steel shaft was used for mixing. A pH controller was used to control the pH value of the solution by adding 0.1 M HNO_3 or NaOH solution into the reactor. Hydrogen peroxide was supplied by a syringe pump with a constant feed rate.

The effect of the pH value of the solution on the system performance was studied at various pH values of 2.0, 2.5, 3.0, and 4.0 with a constant dosage rate of H_2O_2 of 1.99×10^{-4} mol/min-L and an initial BOF slag dose of 20 g/L and PEG dose of 30 mg/L, respectively. The influence of the UV intensity on the system performance was evaluated at various UV intensities with 2.49×10^{-4} mol/min-L hydrogen peroxide, 20 g/L of BOF slag, and 30 mg/L of PEG at a pH value of 2.5. The effect of hydrogen peroxide was examined by dosing it at various dosage rates (9.97×10^{-5} , 1.50×10^{-4} , 1.99×10^{-4} , 2.49×10^{-4} , 2.99×10^{-4} , and 3.98×10^{-4} mol/min-L) into the reactor with a $120 \mu\text{W}/\text{cm}^2$ UV intensity, 20 g/L of BOF slag, and 30 mg/L of PEG at a pH value

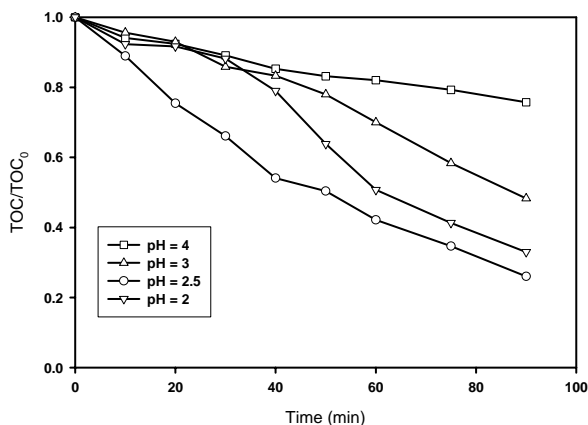


Fig. 2. Dependence of the mineralization of PEG on time under various pH values adjusted by means of HNO₃. Experimental conditions: initial concentration of PEG (C_{PEG0}) = 30 mg/L, initial concentration of BOF slag (C_{BOF}) = 20 g/L, dosing rate of H₂O₂ ($dC_{H_2O_2}/dt$) = 1.99×10^{-4} mol/min-L, UV intensity = 120 μ W/cm², $T = 298$ K.

of 2.5. The effect of BOF slag was studied at various initial concentrations of 5, 10, 15, 20, 25, and 30 g/L with a 120 μ W/cm² UV intensity, 2.49×10^{-4} mol/min-L of hydrogen peroxide, and 30 mg/L of PEG at a pH value of 2.5. The temperature in each of the above experiments was maintained at 25°C. The effect of the temperature was evaluated at 15, 25, and 35°C with a 120 μ W/cm² UV intensity, 20 g/L of BOF slag, 2.49×10^{-4} mol/min-L of hydrogen peroxide, and 30 mg/L of PEG at a pH value of 2.5.

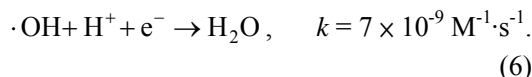
RESULTS AND DISCUSSION

Effects of pH

As BOF slag was placed in the acid solution, some of its metallic oxides dissolved into the solution. Therefore, ferrous ions (Fe²⁺) could be generated from the BOF slag in the acid solution and participated in the Fenton reaction. As described in our previous work concerning the degradation of 2-naphthalenesulfonate (Chiou *et al.*, 2004a), the leachate concentration of Fe²⁺ was affected by the pH value of the solution. Also, the pH value was previously found to be a parameter that affected a photo-Fenton reaction (McGinnis *et al.*, 2000). As shown in Fig. 2, the mineralization efficiencies of TOC_{PEG} , $\eta_{TOC,PEG} = (TOC_0 - TOC)/TOC_0$, were only 51.7% and 24.3% at pH 3 and 4, respectively, after 90 min of reaction time (t). The lower mineralization efficiencies were due to the formation of iron hydroxide precipitation and a lower leachate concentration of iron ions from BOF slag under a higher pH value.

$\eta_{TOC,PEG}$ increased with acidity (decreasing pH value) up to a pH value of 2.5 but decreased with a

further increase in acidity. The $\eta_{TOC,PEG}$ values were about 74.1% and 64.3% for pH values of 2.5 and 2, respectively, at $t = 90$ min. Previous studies on the Fenton process (Lin and Lo, 1997; Wanpeng *et al.*, 1996) found that the optimal pH value condition for a Fenton reaction was pH = 3, suggesting that H⁺ in solutions at very low pH values may react with \cdot OH, as described by Eq. (6), and form H₂O (Lin and Lo, 1997):



Hence, excess H⁺ under very low pH conditions can consume \cdot OH in the solution, thus degrading the decomposition performance of \cdot OH for the target organic compounds. However, the role of the pH value suggested in previous studies (Lin and Lo, 1997; Wanpeng *et al.*, 1996) was based on experiments performed with the single-dose addition of H₂O₂ and Fe²⁺ at the beginning. In the present study, Fe²⁺ was leached out continuously from the BOF slag. Hence, to evaluate the effect of the pH value, we considered the inhibition described by Eq. (6) as well as the effect of the amount of Fe²⁺ leached out from the BOF slag at lower pH values on the efficiency of the Fenton reaction. Lower pH values of the solution led to larger amounts of Fe²⁺ leached out during the Fenton reaction, but the higher acidity of the solution could reduce the mineralization efficiency of the Fenton reaction, according to Eq. (6). Moreover, Fe(OH)²⁺ was reported to be the dominant species in the Fe³⁺-hydroxyl complex in aqueous solutions with pH values ranging from 2.5 to 5 (Wu and Deng, 2000), and here, the lower quantity of Fe(OH)²⁺ resulted in lower concentrations of Fe²⁺ and \cdot OH via Eq. (3). When pH < 2.5, the concentration of Fe(OH)²⁺ was very low in the aqueous solution, which subsequently contributed lower concentration of Fe²⁺ and \cdot OH, and then lower $\eta_{TOC,PEG}$. Thus, the optimal pH value for the effective mineralization of PEG was found to be 2.5. In order to achieve better treatment efficiency, the pH value of solution was maintained at 2.5 in the following experiments.

Mineralization efficiency of PEG under various conditions

The wavelength of radiation is an important parameter for the production of Fe²⁺ and hydroxyl radicals from the Fe³⁺-hydroxyl complex in aqueous solutions via the photolytic reaction (Benkelberg and Warneck, 1995; Nadtochenko and Kiwi, 1998; Wu and Deng, 2000). Fe(OH)²⁺ is the dominant species in aqueous solutions with pH values ranging from 2.5 to 5 (Wu and Deng, 2000), and wavelengths of UV radiation ranging from 290 to 400 nm can

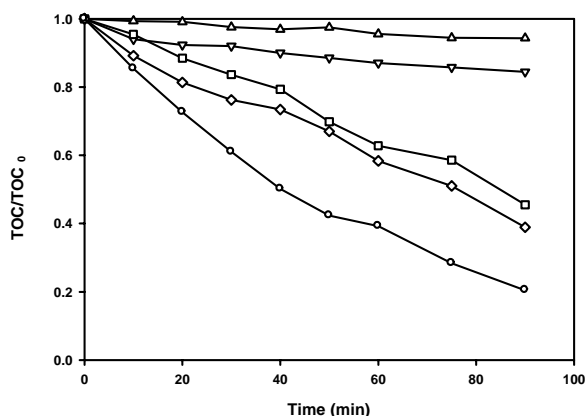


Fig. 3. Dependence of the mineralization of PEG on time under various conditions. (Δ): no BOF, UV intensity = $120 \mu\text{W}/\text{cm}^2$, $dC_{\text{H}_2\text{O}_2}/dt = 1.99 \times 10^{-4} \text{ mol}/\text{min}\cdot\text{L}$; (∇): no H_2O_2 , UV intensity = $120 \mu\text{W}/\text{cm}^2$, $C_{\text{BOF}} = 25 \text{ g}/\text{L}$; (\square): no UV, $C_{\text{BOF}} = 25 \text{ g}/\text{L}$, $dC_{\text{H}_2\text{O}_2}/dt = 1.99 \times 10^{-4} \text{ mol}/\text{min}\cdot\text{L}$; (\diamond): photon-Fenton, UV intensity = $60 \mu\text{W}/\text{cm}^2$, $C_{\text{BOF}} = 25 \text{ g}/\text{L}$, $dC_{\text{H}_2\text{O}_2}/dt = 1.99 \times 10^{-4} \text{ mol}/\text{min}\cdot\text{L}$; (\circ): photon-Fenton, UV intensity = $120 \mu\text{W}/\text{cm}^2$, $C_{\text{BOF}} = 25 \text{ g}/\text{L}$, $dC_{\text{H}_2\text{O}_2}/dt = 1.99 \times 10^{-4} \text{ mol}/\text{min}\cdot\text{L}$. $C_{\text{PEG0}} = 30 \text{ mg}/\text{L}$, $\text{pH} = 2.5$, and $T = 298 \text{ K}$ in all of the experiments.

photolysis $\text{Fe}(\text{OH})^{2+}$ to produce Fe^{2+} and hydroxyl radical based on the charge transfer band of $\text{Fe}(\text{OH})^{2+}$ as indicated in Eq. (3). Furthermore, according to a report by Pignatello (1992), the degradation of organic compound by $\text{Fe}^{3+}/\text{H}_2\text{O}_2$ was accelerated by irradiation with light wavelengths above 300 nm. Therefore, the wavelength of UV radiation utilized in this study was kept within a range from 300 to 400 nm. In general, the most readily available UV lamps with maximum emitting wavelengths ranging from 300 to 400 nm are 312 and 360 nm lamps. Pignatello (1992) also indicated that a radiation wavelength of 312 nm led to a higher quantum yield than did a wavelength of 360 nm. Moreover, the direct photolysis of H_2O_2 generates $\cdot\text{OH}$ according to Eq. (5), requiring UV radiation wavelengths $< 360 \text{ nm}$ (El-Morsi *et al.*, 2002). Therefore, a UV radiation wavelength of 312 nm was investigated in this study.

Figure 3 presents $\eta_{\text{TOC,PEG}}$ as a function of time under different conditions. Condition (a) denotes a reaction system with a UV intensity of $120 \mu\text{W}/\text{cm}^2$ and a $dC_{\text{H}_2\text{O}_2}/dt$ value of $1.99 \times 10^{-4} \text{ mol}/\text{min}\cdot\text{L}$ but without BOF slag here (called UV/ H_2O_2). The obtained $\eta_{\text{TOC,PEG}}$ percentage was only 6.7% after 90 min of treatment. This result indicated that the direct UV photolysis of PEG and the oxidation of PEG by hydroxyl radicals shown in Eq. (5) did not lead to significant mineralization. Condition (b) represents a reaction system with a UV intensity of $120 \mu\text{W}/\text{cm}^2$ and an initial BOF slag concentration C_{BOF} of 25 g/L but without H_2O_2 (denoted here as

UV/BOF slag). The percentage of $\eta_{\text{TOC,PEG}}$ was about 16% after 90 min of reaction time. This result revealed that the observed mineralization of PEG was due to oxidation by $\cdot\text{OH}$ shown in Eq. (3). Under condition (c), with H_2O_2 and BOF slag but without UV (denoted here as $\text{H}_2\text{O}_2/\text{BOF}$ slag), the Fe^{2+} leached from the BOF slag mixed with H_2O_2 and initiated the Fenton reaction. In this case, a better efficiency for $\eta_{\text{TOC,PEG}}$ (about 50% at $t = 90 \text{ min}$) was achieved than under conditions (a) and (b), verifying the strong oxidation ability of the basic Fenton reaction. Conditions (d) with UV ($60 \mu\text{W}/\text{cm}^2$) / $\text{H}_2\text{O}_2/\text{BOF}$ slag and (e) with UV ($120 \mu\text{W}/\text{cm}^2$) / $\text{H}_2\text{O}_2/\text{BOF}$ slag led to efficient mineralization in the photo-Fenton reaction. The experimental results showed that the introduction of UV light enhanced $\eta_{\text{TOC,PEG}}$, indicating that higher UV intensity resulted in higher $\eta_{\text{TOC,PEG}}$. According to Eqs. (3), (4), and (5), UV irradiation can promote the production of Fe^{2+} and hydroxyl radicals, and Fe^{2+} mixed with H_2O_2 can initiate the Fenton reaction, thus increasing the efficiency of mineralization of PEG. As a result, the mineralization efficiency of PEG under various conditions follows the sequence: UV ($120 \mu\text{W}/\text{cm}^2$) / $\text{H}_2\text{O}_2/\text{BOF}$ slag $>$ UV ($60 \mu\text{W}/\text{cm}^2$) / $\text{H}_2\text{O}_2/\text{BOF}$ slag $>$ $\text{H}_2\text{O}_2/\text{BOF}$ slag $>$ UV ($120 \mu\text{W}/\text{cm}^2$) /BOF slag $>$ UV ($120 \mu\text{W}/\text{cm}^2$) / H_2O_2 .

Effects of the ratio of $\text{H}_2\text{O}_2/\text{BOF}$ slag

Previous works (Tang and Huang, 1996; Tang and Tassos, 1997) reported that an appropriate ratio of H_2O_2 to Fe^{2+} was needed to achieve the optimal treatment efficiency for organic compounds. However, the optimal ratio varied with the characteristics of the organics. The photo-Fenton process adopted in this study employed BOF slag, which supplies Fe^{2+} at a constant leaching rate. Hence, the proper continuous addition of H_2O_2 can result in an adequate ratio of $\text{H}_2\text{O}_2/\text{Fe}^{2+}$ with constant supplementation of Fe^{2+} from BOF slag.

The effects of various dosing rates of H_2O_2 ($dC_{\text{H}_2\text{O}_2}/dt$) on $\eta_{\text{TOC,PEG}}$ are shown in Fig. 4. $\eta_{\text{TOC,PEG}}$ increased as $dC_{\text{H}_2\text{O}_2}/dt$ increased from 9.97×10^{-5} to $2.49 \times 10^{-4} \text{ mol}/\text{min}\cdot\text{L}$ but then decreased $dC_{\text{H}_2\text{O}_2}/dt$ exceeded $2.49 \times 10^{-4} \text{ mol}/\text{min}\cdot\text{L}$. This transition was due to the effect of the ratio of H_2O_2 to Fe^{2+} on $\eta_{\text{TOC,PEG}}$. At higher H_2O_2 and Fe^{2+} concentrations, the production of $\cdot\text{OH}$ increased, acting as the sources of the reactions with hydroxyl radicals. An adequate increase in the production of $\cdot\text{OH}$ should correspond to an increase in the mineralization of PEG. However, the reaction rate constant between H_2O_2 and $\cdot\text{OH}$ (reaction in Eq. (7)) (Buxton *et al.*, 1988) was as high as $2.7 \times 10^7 \text{ M}^{-1}\cdot\text{s}^{-1}$:

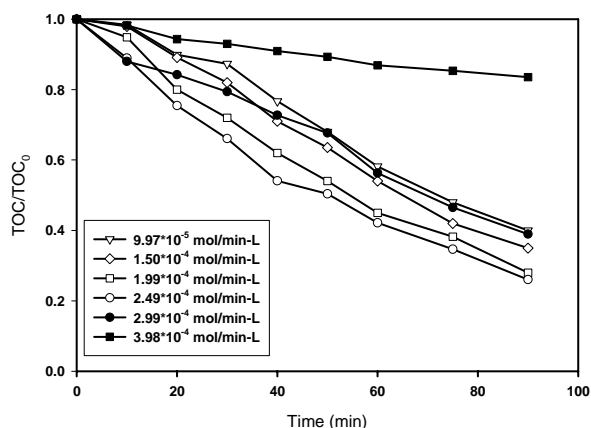


Fig. 4. Dependence of the mineralization of PEG on time under various H₂O₂ dosing rates. Experimental conditions: $C_{PEG0} = 30$ mg/L, UV intensity = $120 \mu\text{W}/\text{cm}^2$, $C_{BOF} = 20$ g/L, $T = 298$ K, pH = 2.5.

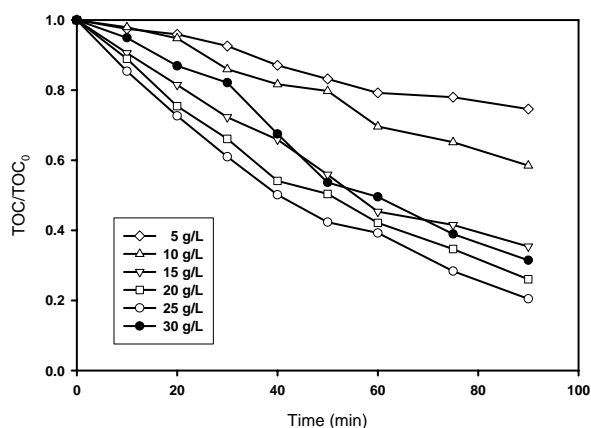
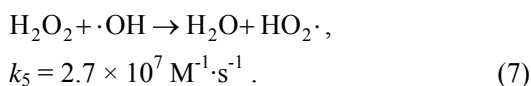


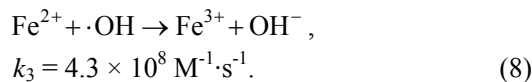
Fig. 5. Time variation of the mineralization of PEG under various C_{BOF} values. Experimental conditions: UV intensity = $120 \mu\text{W}/\text{cm}^2$, $C_{PEG0} = 30$ mg/L, a dosing rate of $\text{H}_2\text{O}_2 = 2.49 \times 10^{-4}$ mol/min-L, $T = 298$ K, pH = 2.5.



Thus, reaction (7) became a predominant reaction in comparison with the reaction between $\cdot\text{OH}$ and PEG at higher concentrations of H_2O_2 , resulting in the large consumption of $\cdot\text{OH}$ with excess H_2O_2 instead of the utilization of $\cdot\text{OH}$ in decomposing PEG. Hence, an increase in the concentration of a scavenger, such as H_2O_2 , can result in an increase in the scavenging rate of radicals and, thus, a reduction in the mineralization efficiency. In this study, the predominant reaction of $\cdot\text{OH}$ with H_2O_2 thus resulted in lower $\eta_{\text{TOC,PEG}}$ values when $dC_{\text{H}_2\text{O}_2}/dt$ was higher than 2.49×10^{-4} mol/min-L.

The effects of the loading concentrations of BOF slag on the mineralization of PEG are shown in Fig. 5. The results indicate that a higher $\eta_{\text{TOC,PEG}}$ value could be obtained with a higher C_{BOF} (the

amount of BOF slag per volume of solution) value up to 25 g/L. However, the $\eta_{\text{TOC,PEG}}$ value decreased when C_{BOF} was higher than 25 g/L in this study. This was due to the fact that the excess Fe^{2+} in the solution consumed the $\cdot\text{OH}$ in the solution, as shown in Eq. (8) (Tang and Tassos, 1997), which reduced the oxidation efficiency:



The experimental results obtained in this study suggest that a $dC_{\text{H}_2\text{O}_2}/dt$ value of 2.49×10^{-4} mol/min-L and a C_{BOF} value of 25 g/L in a solution at pH = 2.5 are the operating operation conditions for the mineralization of PEG.

Kinetic studies of PEG mineralization

The reaction kinetic of a photo-Fenton reaction on the mineralization of PEG via BOF slag with UV/H₂O₂ can be described as

$$\frac{dC}{dt} = -kC^m, \quad (9)$$

where C , m , t , and k represent the TOC concentration of PEG, the order of the reaction, the time, and the reaction rate constant, respectively. For a first-order reaction, Eq. (9) becomes

$$\ln\left(\frac{C}{C_0}\right) = -kt, \quad (10)$$

where C_0 is the initial TOC concentration of PEG.

Consider the experimental data shown in Figs. 4 and 5, with $dC_{\text{H}_2\text{O}_2}/dt$ and C_{BOF} values ranging from 9.97×10^{-5} to 2.49×10^{-4} mol/min-L and 5 to 25 g/L, respectively, and where the $\eta_{\text{TOC,PEG}}$ value increased as the dosages of H_2O_2 and BOF slag increased. Figure 6(a) shows plots at various $dC_{\text{H}_2\text{O}_2}/dt$ values for a solution with $C_{BOF} = 20$ g/L. Figure 6(b) shows plots at various C_{BOF} with $dC_{\text{H}_2\text{O}_2}/dt$ at 2.49×10^{-4} mol/min-L H_2O_2 . The results of Figs. 6(a) and 6(b) revealed reasonably good linear fits of the first-order kinetic model, as described in Eq. (10).

The value of the slope or k in Fig. 6 varied with the $dC_{\text{H}_2\text{O}_2}/dt$ and C_{BOF} values, and are further illustrated in Fig. 7. The linear relationships between $\ln k$ with $\ln(dC_{\text{H}_2\text{O}_2}/dt)$ and $\ln C_{BOF}$ give the following correlation:

$$k = k_0(dC_{\text{H}_2\text{O}_2}/dt)^x(C_{BOF})^y. \quad (11)$$

In Eq. (11), $dC_{\text{H}_2\text{O}_2}/dt$, C_{BOF} , x , and y are the molar dosing rate of H_2O_2 (mol/min-L), the loading of BOF slag (g/L), and the orders of concentration dependence of $dC_{\text{H}_2\text{O}_2}/dt$ and C_{BOF} , respectively.

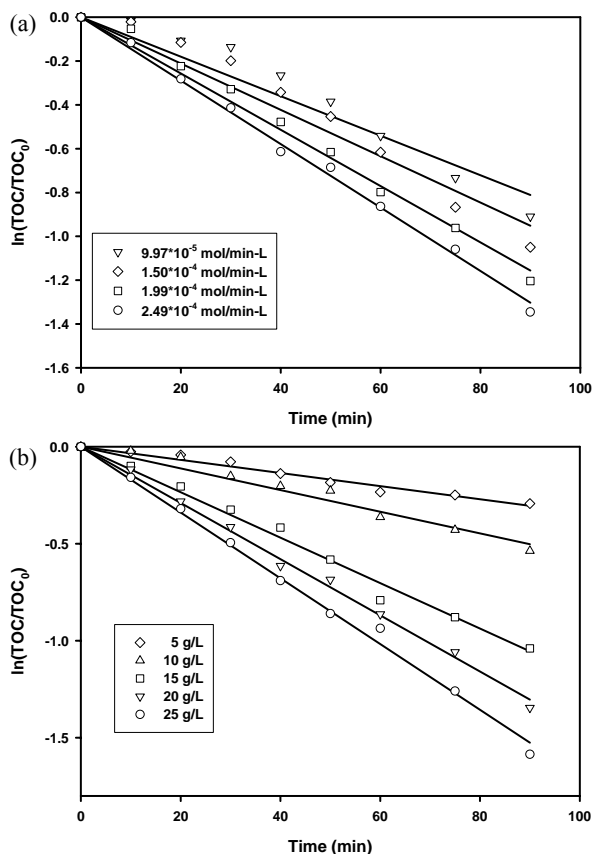


Fig. 6. Analysis of the mineralization kinetics of PEG simulated by means of a first-order reaction. (a) Cases with various H_2O_2 dosing rates at a constant $C_{\text{BOF}} = 20$ g/L. The values of R^2 for the regression lines of ∇ , \diamond , \square , \circ : 0.935, 0.948, 0.989, and 0.996. (b) Cases with various BOF slag loadings at a constant H_2O_2 dosing rate of 2.49×10^{-4} mol/min-L. The R^2 values for the regression lines of \diamond , \triangle , ∇ , \square , and \circ : 0.971, 0.964, 0.988, 0.996, and 0.995, respectively.

The values of x and y obtained from the slopes in Fig. 7 (a) and 7 (b) were 0.53 and 1.06, respectively.

The temperature dependence of the kinetic parameter k_0 in Eq. (12) can be described by the Arrhenius equation:

$$k_0 = A \exp\left(-\frac{Ea}{RT}\right), \quad (12)$$

where A , Ea , T , and R are the frequency factor ($1/\text{min}(\text{mol}/\text{min}\cdot\text{L})^{-0.53}(\text{g}/\text{L})^{-1.06}$), activation energy (J/mol), temperature (K), and gas constant (J/(mol·K)), respectively. The effect of temperature on kinetic parameter k_0 was evaluated at 15, 25, and 35°C, yielding k_0 values of 0.0295, 0.0453, and 0.0751 $1/\text{min}(\text{mol}/\text{min}\cdot\text{L})^{-0.53}(\text{g}/\text{L})^{-1.06}$, respectively. Plotting $\ln k_0$ against $1/T$ (1/K) gave an A value of 3.4×10^9 $1/\text{min}(\text{mol}/\text{min}\cdot\text{L})^{-0.53}(\text{g}/\text{L})^{-1.06}$ and an Ea value of 62.19 kJ/mol. Combining Eqs. (11) and (12) along with the reaction orders, frequency factor, and activated energy yields:

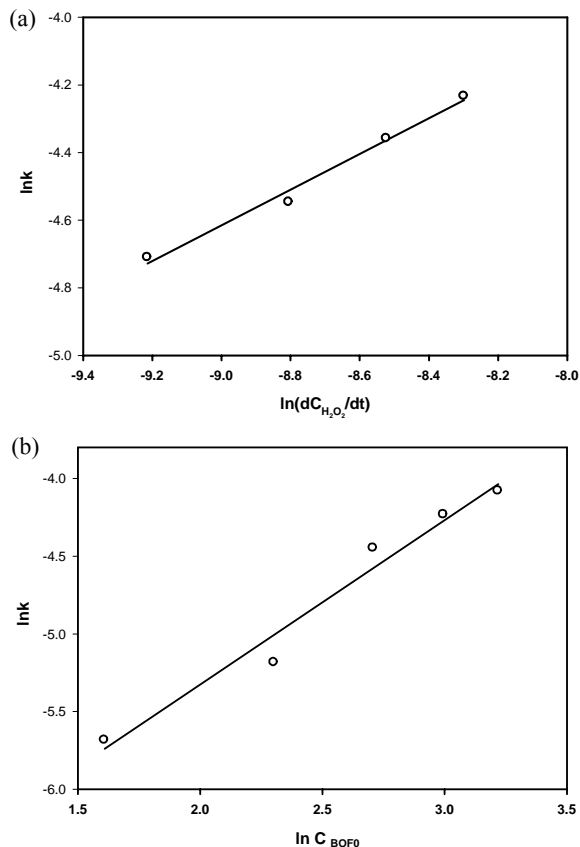


Fig. 7. The relationship of k with $dC_{\text{H}_2\text{O}_2}/dt$ and C_{BOF} . UV intensity = $120 \mu\text{W}/\text{cm}^2$, $T = 298$ K, $\text{pH} = 2.5$. (a) $\ln k$ vs. $\ln(dC_{\text{H}_2\text{O}_2}/dt)$ at a constant $C_{\text{BOF}} = 20$ g/L, $r^2 = 0.988$. (b) $\ln k$ vs. $\ln C_{\text{BOF}}$ at a constant $dC_{\text{H}_2\text{O}_2}/dt = 2.49 \times 10^{-4}$ mol/min-L, $R^2 = 0.970$. Units of k , $dC_{\text{H}_2\text{O}_2}/dt$, and C_{BOF} : 1/min, mol/min-L, and g/L, respectively.

$$k = 3.4 \times 10^9 \exp\left(-\frac{7480}{T}\right) (dC_{\text{H}_2\text{O}_2}/dt)^{0.53} (C_{\text{BOF}})^{1.06}. \quad (13)$$

Figure 8 compares the values of k predicted by Eq. (13) with the experimental data, showing a satisfactory agreement with an R^2 value of 0.994. The reaction rate constant (k) increased with increasing $dC_{\text{H}_2\text{O}_2}/dt$ and C_{BOF} value in the range $9.97 \times 10^{-5} \sim 2.49 \times 10^{-4}$ mol/min-L for $dC_{\text{H}_2\text{O}_2}/dt$ and 5 ~ 25 g/L for C_{BOF} .

CONCLUSION

The major results of applying photo-Fenton with BOF slag to mineralize PEG can be summarized as follows:

- (1) The mineralization efficiency of PEG followed the sequence: UV($120 \mu\text{W}/\text{cm}^2$)/ H_2O_2 /BOF slag > UV($60 \mu\text{W}/\text{cm}^2$)/ H_2O_2 /BOF slag > H_2O_2 /



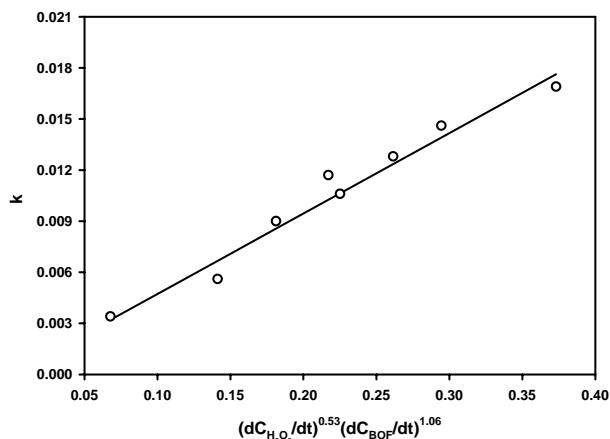


Fig. 8. Reaction rate constant (k) versus $(dC_{H_2O_2}/dt)^{0.63} (C_{BOF})^{0.60}$ for the mineralization of PEG with BOF slag in the presence of UV/H₂O₂. Experimental conditions: $T = 25^\circ\text{C}$ (298 K), UV intensity = 120 $\mu\text{W}/\text{cm}^2$, pH = 2.5. Line: $k = 3.4 \times 10^9 \exp(-7480/T) (dC_{H_2O_2}/dt)^{0.53} (C_{BOF})^{1.06}$, \circ : experimental data, $R^2 = 0.994$.

BOF slag > UV(120 $\mu\text{W}/\text{cm}^2$)/BOF slag > UV(120 $\mu\text{W}/\text{cm}^2$)/H₂O₂.

- (2) The experimental results obtained in this study suggest that UV irradiation of 120 $\mu\text{W}/\text{cm}^2$, a H₂O₂ dosage of 2.49×10^{-4} mol/min-L, and a BOF slag loading of 25 g/L in a solution at pH 2.5 are the optimal operating conditions for the mineralization of PEG, and in this study yielded 79.5% mineralization efficiency during 90 min of reaction time.
- (3) The reaction rate for the decomposition of PEG in terms of TOC (k) can be further correlated with the molar dosing rate of H₂O₂ and the loading concentration of BOF slag by means of power expressions, yielding

$$k = 3.4 \times 10^9 \exp\left(-\frac{7480}{T}\right) (dC_{H_2O_2}/dt)^{0.53} (C_{BOF})^{1.06}.$$

NOMENCLATURE

C_{BOF}	amount of BOF slag in an aqueous solution, g/L
$C_{Fe,2+}$	concentration of ferrous ion in an aqueous solution, mg/L
C_{PEG0}	initial concentration of PEG in an aqueous solution, mg/L

Greek symbol

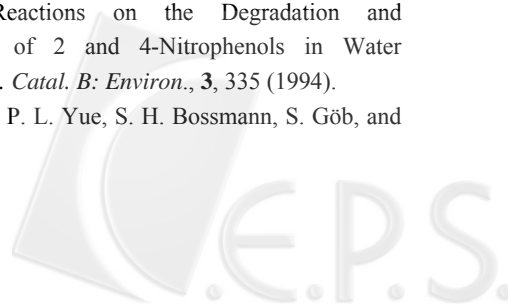
$\eta_{TOC,PEG}$	decomposition efficiency of TOC_{PEG} , $(TOC_{PEG0} - TOC_{PEG})/TOC_{PEG0}$
------------------	---

Acronyms

BOF slag	basic oxygen furnace slag
PEG	polyethylene glycol

REFERENCES

- Bajt, O., G. Mailhot, and M. Bolte, "Degradation of Dibutyl Phthalate by Homogeneous Photocatalysis with Fe(III) in Aqueous Solution," *Appl. Catal. B: Environ.*, **33**, 239 (2001).
- Benkelberg, H. J. and P. Warneck, "Photodecomposition of Iron (III) Hydroxo and Sulfato Complexes in Aqueous Solution: Wavelength Dependence of OH⁻ and SO₄²⁻ Quantum Yields," *J. Phys. Chem.*, **99**, 5214 (1995).
- Buxton, G. V., C. L. Greenstock, W. P. Helman, and A. B. Ross, "Critical Review of Rate Constants for Reactions of Hydrated Electrons, Hydrogen Atoms and Hydroxyl Radicals ($\cdot\text{OH}/\text{O}^-$) in Aqueous Solution," *J. Phys. Chem. Data*, **17**, 513 (1988).
- Chen, R. and J. J. Pignatello, "Role of Quinone Intermediates as Electron Shuttles in Fenton and Photoassisted Oxidation of Aromatic Compounds," *Environ. Sci. Technol.*, **31**, 1862 (1997).
- Chiou, C. S., F. C. Chang, C. Y. Chang, C. T. Chang, and Y. S. Li, "Degradation of 2-Naphthalenesulfonate in Aqueous Solution by Hydrogen Peroxide in the Presence of Basic Oxygen Furnace Slag," *J. Chin. Inst. Chem. Engrs.*, **35**(4), 417 (2004a).
- Chiou, C. S., F. C. Chang, C. Y. Chang, Y. P. Wu, C. T. Chang, Y. S. Li, and Y. H. Chen, "Mineralization of Polyethylene Glycol in Aqueous Solution by Hydrogen Peroxide with Basic Oxygen Furnace Slag," *Environ. Technol.*, **25**, 1357 (2004b).
- Chou, S. S., C. P. Huang, and Y. H. Huang, "Heterogeneous and Homogeneous catalytic Oxidation by Supported γ -FeOOH in a Fluidized-Bed Reactor: Kinetic Approach," *Environ. Sci. Technol.*, **35**, 1247 (2001).
- El-Morsi, T. M., M. M. Emara, H. M. H. Abd El Bary, A. S. Abd-El-Aziz, and K. J. Friesen, "Homogeneous Degradation of 1,2,9,10-Tetrachlorodecane in Aqueous Solutions Using Hydrogen Peroxide, Iron and UV Light," *Chemosphere*, **47**, 343 (2002).
- Feng, J., X. Hu, P. L. Yue, H. Y. Zhu, and G. Q. Lu, "Discoloration and Mineralization of Reactive Red HE-3B by Heterogeneous Photo-Fenton Reaction," *Water Res.*, **37**, 3776 (2003).
- Kiwi, J., C. Pulgarin, and P. Peringer, "Effect of Fenton and Photo-Fenton Reactions on the Degradation and Biodegradability of 2 and 4-Nitrophenols in Water Treatment," *Appl. Catal. B: Environ.*, **3**, 335 (1994).
- Lei, L. C., X. J. Hu, P. L. Yue, S. H. Bossmann, S. Göb, and



- A. M. Braun, "Oxidative Degradation of Polyvinyl Alcohol by the Photochemically Enhanced Fenton Reaction," *J. Photochem. Photobiol. A: Chem.*, **116**, 159 (1998).
- Li, Y. S., "The Use of Waste Basic Oxygen Furnace Slag and Hydrogen Peroxide to Degrade 4-Chlorophenol," *Waste Manage.*, **19**, 495 (1999).
- Lin, S. H. and C. C. Lo, "Fenton Process for Treatment of Desizing Wastewater," *Water Res.*, **31**, 2050 (1997).
- Lin, S. S. and M. D. Gurol, "Catalytic Decomposition of Hydrogen Peroxide on Iron Oxide: Kinetic, Mechanism, and Implications," *Environ. Sci. Technol.*, **32**, 1417 (1998).
- Liou, M. J., M. C. Lu, and J. N. Chen, "Oxidation of TNT by Photo-Fenton Process," *Chemosphere*, **57**, 1107 (2004).
- McGinnis, B. D., V. D. Adams, and E. J. Middlebrooks, "Degradation of Ethylene Glycol in Photo Fenton Systems," *Water Res.*, **34**, 2346 (2000).
- Nadtochenko, V. A. and J. Kiwi, "Photolysis of FeOH^{2+} and FeCl^{2+} in Aqueous Solution, Photodissociation Kinetics and Quantum Yields," *Inorg. Chem.*, **37**, 5233 (1998).
- Plgnatello, J. J., "Dark and Photoassisted Fe^{3+} -Catalyzed Degradation of Chlorophenoxy Herbicides by Hydrogen Peroxide," *Environ. Sci. Technol.*, **26**, 944 (1992).
- Rivas, F. J., F. T. Beltran, J. Frades, and P. Buxeda, "Oxidation of *p*-Hydroxybenzoic Acid by Fenton's Reagent," *Water Res.*, **35**(2), 387 (2001).
- Saxe, J. K., H. E. Allen, and G. R. Nicol, "Fenton Oxidation of Polycyclic Aromatic Hydrocarbons after Surfactant-Enhanced Soil Washing," *Environ. Eng. Sci.*, **17**(2), 233 (2000).
- Tang, W. Z. and C. P. Huang, "An Oxidation Kinetic Model of Unsaturated Chlorinated Aliphatic Compounds by Fenton's Reagent" *J. Environ. Sci. Health A*, **31**, 2755 (1996).
- Tang, W. Z. and S. Tassos, "Oxidation Kinetic and Mechanisms by Fenton's Reagent," *Water Res.*, **31**, 1117 (1997).
- Tuba, T. E. and M. D. Gurol, "Oxidation of Diethylene Glycol with Ozone and Modified Fenton Process," *Chemosphere*, **47**, 293 (2002).
- Walling, C., "Fenton's Reagent Revisited," *Accounts Chem. Res.*, **8**, 125 (1975).
- Wanpeng, Z., Y. Zhihua, and W. Li, "Application of Ferrous-Hydrogen Peroxide for the Treatment of H-Acid Manufacturing Process Wastewater," *Water Res.*, **30**, 2949 (1996).
- Watts, R. J., A. P. Jones, P. H. Chen, and A. Kenny, "Mineral-Catalyzed Fenton-Like Oxidation of Sorbed Chlorobenzenes," *Water Environ. Res.*, **69**(3), 269 (1997).
- Wu, F. and N. Deng, "Photochemistry of Hydrolytic Iron (III) Species and Photoinduced Degradation of Organic Compounds. A Minireview," *Chemosphere*, **41**, 1137 (2000).
- Zhao, X. K., G. P. Yang, Y. J. Wang, and X. C. Gao, "Photochemical Degradation of Dimethyl Phthalate by Fenton Reagent," *J. Photochem. Photobiol. A: Chem.*, **161**, 215 (2004).

(Manuscript received Dec., 14, 2005, and accepted May, 16, 2006)

煉鋼廢棄物結合UV/H₂O₂以分解水溶液中之聚乙烯醇

邱求三

國立宜蘭大學環境工程學系

陳奕宏

國立高雄應用科技大學化學與材料工程學系

張慶源

國立台灣大學環境工程學研究所

謝哲隆 劉鎮宗 張章堂

國立宜蘭大學環境工程學系

摘要

煉鋼廢棄物中之轉爐石其富含 Fe^{2+} ，可應用來催化雙氧水以啟動費頓反應，進而產生氫氧自由基來礦化有機污染物，費頓反應後所產生之 Fe^{3+} 可藉由紫外光的照射而轉換成 Fe^{2+} ，如此便可持續催化雙氧水，且紫外光亦可分解雙氧水以產生氫氧自由基，進而提升有機物礦化的效率，本實驗便利用轉爐石於UV/H₂O₂的存在下以礦化水溶液中的聚乙烯醇，實驗發現在pH = 2.5、UV光強度為120 $\mu\text{W}/\text{cm}^2$ ，雙氧水及轉爐石添加量分別為 2.49×10^{-4} mol/min-L及25 g/L時，於90分鐘之反應時間，對PEG可達79.5%的最佳礦化效率，並將此礦化效率以動力學的方式加以描述。

